

DUAL DISCRETIZATION METHOD FOR SEMICONDUCTOR DEVICE SIMULATOR*

Toshiaki KOJIMA, Yoshifuru SAITO and Ryo DANG

Graduate School of Engineering, Hosei University 3-7-2 Kajino-cho, Koganei, Tokyo 184, Japan

Received 1990

We propose a new mathematical model for simulating a semiconductor device. The model is formulated based on a discretization method using a Voronoi-Delaunay (VD) diagram. The fact that the VD diagram consists of two mesh systems, independent but geometrically orthogonal to each other, leads to two completely different sets of formulae. We apply the method to a conventional MOSFET DC analysis as an initial test example. We found that the new method provides similar results compared to a conventional one. This confirmed the validity of our new formulation.

1. Introduction

For analyzing semiconductor devices, numerical techniques are successfully introduced and implemented [1-3]. In the case of calculating a two- or three-dimensional problem, space discretization is very important whether to apply a finite difference method (FDM) or a finite element method (FEM).

Recently, the dual discretization methods based on the Voronoi-Delaunay diagram have been effectively employed in the analysis of electric and/or magnetic fields [4-6]. Basically, these methods utilize the local orthogonality between each edge pair, one edge of a Delaunay triangle and one of a Voronoi polygon, to form a set of coordinates upon which the formulation is implemented. The boundary condition is different in the case of using the Delaunay triangle mesh system to that of using the Voronoi polygon mesh system.

In a previous paper [7], the Poisson equation is discretized by both methods for analyzing a reverse-biased P-N junction. Both solutions so obtained show good agreement with each other. In contrast to the previous paper where the device under investigation is composed of only one kind of material, the present paper deals

with a MOSFET which is formed basically of two different materials with separate permittivities, namely, silicon(Si) and silicon dioxide(SiO₂). Furthermore, in addition to the Poisson equation, two current continuity equations, one for electrons and one for holes, are also considered in the present case. In other words, in contrast to the previous case of zero current flow, the present case deals with the general situation where a non-zero current is existent in the device under consideration. In this paper, the five-point FDM is applied to both systems. The five nodes for the Delaunay system include a center node and four surrounding adjacent nodes. The formulation for this case is based on a conventional Taylor expansion. On the other hands, the five nodes for the Voronoi system consist of a center node and four surrounding "intermediate" nodes. These "intermediate" nodes are necessary because of the existence of an interface between different materials at the middle of the Voronoi nodes. The application of these "intermediate" nodes is new in the field of the semiconductor device simulation.

2. Dual discretization method

2.1. Equations to be solved

Generally, in the analysis of semiconductor DC characteristics, Poisson equation and two

* Presented at the Second International Symposium on Applied Electromagnetics in Materials, Kanazawa, Japan, 9-11 January, 1990.

current continuity equations (for electrons and holes) are governing equations. The three equations are written as follows.

Poisson equation:

$$\nabla^2 \psi = -\frac{q}{\epsilon} (p - n + N_D - N_A). \quad (1)$$

Current Continuity equations:

(1) Electrons

$$\nabla J_n = -\nabla(q\mu_n n \nabla \psi - qD_n \nabla n) = -q \cdot GR_n. \quad (2)$$

(2) Holes

$$\nabla J_p = -\nabla(q\mu_p p \nabla \psi - qD_p \nabla p) = -q \cdot GR_p. \quad (3)$$

ψ , q , ϵ , N_D and N_A in Poisson equation denote potential, permittivity, electron charge, donor and acceptor concentrations, respectively. On the other hand, $J_{n,p}$, $\mu_{n,p}$, $D_{n,p}$, $GR_{n,p}$ in the current continuity equations denote current densities, mobilities, diffusion constants, and generation-recombination rates, respectively. Note that subscripts n, p refer to electrons and holes, respectively. Also, p and n are hole and electron densities which are described as follows.

$$n = n_i \exp\left[\frac{q}{kT} (\phi_n - \psi)\right], \quad (4)$$

$$p = n_i \exp\left[\frac{q}{kT} (\psi - \phi_p)\right], \quad (5)$$

where n_i , k , T are intrinsic carrier concentration, Boltzmann constant, temperature, ϕ_p and ϕ_n are quasi-Fermi levels for holes and electrons, respectively.

Equations (1)–(5) are numerically solved using a FDM and Gummel's algorithm [8].

2.2. Geometrical duality

Figure 1 indicates a part of the discretized region using a Voronoi–Delaunay diagram. The problem of how to construct this diagram has been explained in details elsewhere (for example [4]) and will not be repeated here. The Delaunay triangles are shown by solid lines. The Voronoi polygons associated with these Delaunay triangles are shown by dashed lines. It can be seen that the Delaunay triangles and the Voronoi polygons are locally orthogonal: each triangle

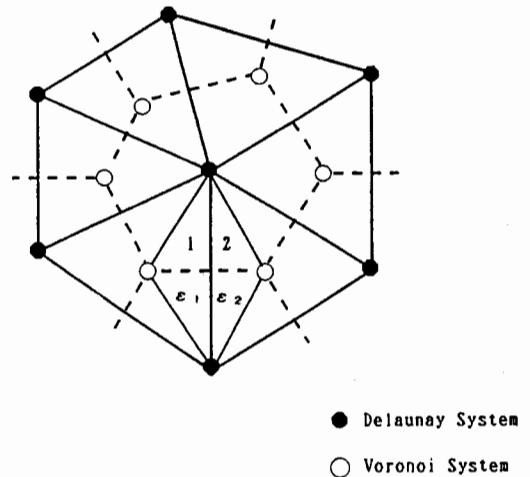


Fig. 1. Voronoi–Delaunay diagram.

edge is perpendicular to the corresponding Voronoi polygon edge. Thus, two complete but independent sets of nodal variables may be defined on this Voronoi–Delaunay diagram: one is located at the vertices of the Delaunay triangles; and the other is located at the vertices of the Voronoi polygons. The governing equations (1), (2), (3) are, therefore, proposed here to be discretized either by the Delaunay or the Voronoi mesh systems, independently.

2.3. Boundary condition

In a MOSFET geometry, one of the most important things is the treatment of the boundary between the gate oxide and the substrate silicon. In order to model this in a reasonable manner, let us consider a locally orthogonal coordinate in the Voronoi Delaunay diagram shown in fig. 2. Each Delaunay triangle adjacent to the boundary has a different medium parameter, permittivity, either ϵ_{ox} or ϵ_{si} . This proves that if considering the locally orthogonal coordinate constructed by a Voronoi polygon's and Delaunay triangle's edge as shown in fig. 2, one can find that the boundary conditions are different whether Delaunay system or Voronoi system is selected. Then we consider the condition for Poisson equation. For Delaunay system (y -direction), the boundary condition at interface be-

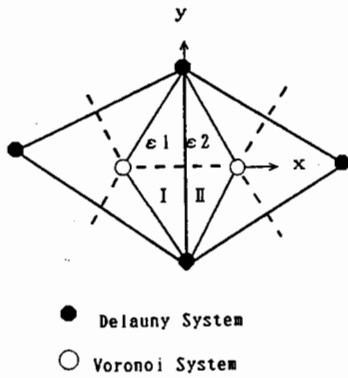


Fig. 2. A locally orthogonal coordinate system in the Voronoi-Delaunay diagram.

tween area 1 and area 2 is that the transversal component of electric field strength is continuous, so that

$$\frac{\partial \psi}{\partial y} \Big|_{\text{area 1}} = \frac{\partial \psi}{\partial y} \Big|_{\text{area 2}} \quad (6)$$

at the gate oxide interface. On the other side, for Voronoi system (*x*-direction), the boundary condition between area 1 and area 2 is that the transversal component of electric flux density is

continuous, so that

$$\epsilon_1 \frac{\partial \psi}{\partial x} \Big|_{\text{area 1}} = \epsilon_2 \frac{\partial \psi}{\partial x} \Big|_{\text{area 2}} \quad (7)$$

at the interface.

For the boundary condition of current continuity equation, J_n and J_p are not continuous from substrate silicon to gate oxide. It means that J_n and J_p do not flow in oxide but in silicon only. So the boundary condition for the Voronoi system is that J_n and J_p are reflective at the interface. The boundary condition for the Delaunay system is that the transversal component of J_n and J_p is non-zero only in one material. For this reason, the formulation for the current continuity equations does not change between two systems. However, the formulation for Poisson equation is not identical for both systems. This formulation is described in detail in the following.

2.4. Formulation using finite difference method

For convenience of comparison with a conventional simulation [1], we have selected a

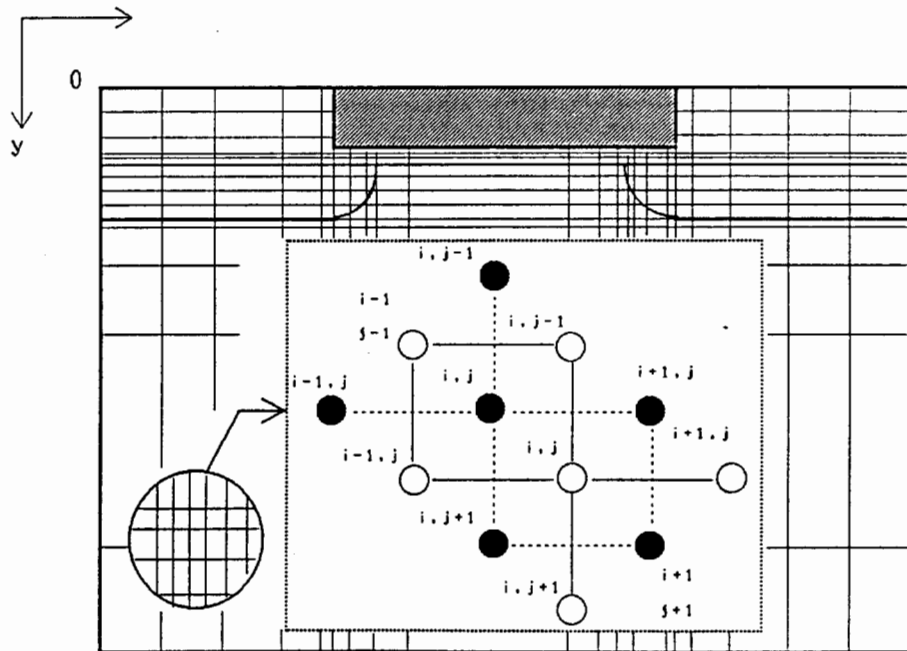


Fig. 3. Interlaced grid structure. Delaunay and Voronoi systems represented by ● and ○ nodes, respectively.

nonuniform, rectangular, interlaced grid form shown by the inset of fig. 3. In this configuration, the Delaunay mesh system and the Voronoi mesh system are located at different sets of grid points alternate to each others. The device is divided into horizontal and vertical regions where ratios between adjacent grid spaces are kept constant. Especially for simulating a MOS-FET device, the mesh numbers at interface between oxide and silicon and the P-N junctions are increased to cope with the drastic variation of potentials and carrier densities at these locations. The interface between the gate oxide and the substrate silicon is chosen to coincide with the Delaunay grid points.

2.4.1. Formulation for Delaunay system

Fig. 4. shows the five-point difference grid for Delaunay system in the general case. Because the material boundary is on the solid line, the region is divided into four blocks with different permittivities denoted by $\epsilon_1 \sim \epsilon_4$.

Poisson equation (1) is integrated using Gauss's theorem, as follows.

$$\int \epsilon \frac{\partial \psi}{\partial x} dy + \int \epsilon \frac{\partial \psi}{\partial x} dx + \int_s \rho dx dy. \quad (8)$$

The 1st order derivative of ψ is described using the forward finite difference for the north direction as follows.

$$\frac{\partial \psi}{\partial y} = \frac{\psi_N - \psi_X}{dy_j}. \quad (9)$$

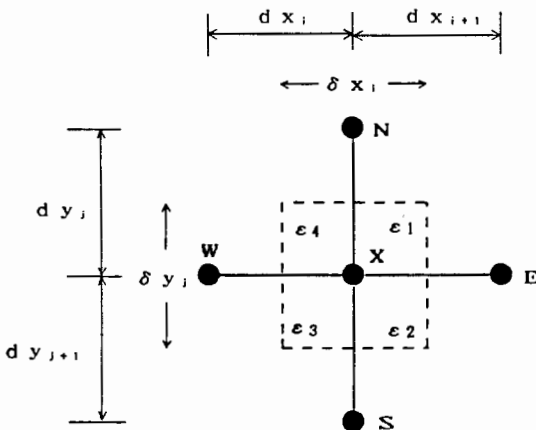


Fig. 4. The coordinate for 5-point FDM in Delaunay system.

A similar derivation is repeated for the other directions of east, south and west. Finally, we arrive at the following formula for the Poisson equation.

$$\begin{aligned} & \frac{1}{2} \left\{ (\epsilon_4 dx_{i+1} + \epsilon_1 dx_i) \frac{\psi_N - \psi_X}{dy_j} \right. \\ & + (\epsilon_3 dy_j + \epsilon_4 dy_{j+1}) \frac{\psi_W - \psi_X}{dx_i} \\ & + (\epsilon_1 dx_{i+1} + \epsilon_2 dy_1) \frac{\psi_E - \psi_X}{dy_j} \\ & \left. + (\epsilon_3 dy_j + \epsilon_2 dy_{j+1}) \frac{\psi_S - \psi_X}{dx_i} \right\} \\ & = \rho \delta x_i \delta y_j. \end{aligned} \quad (10)$$

The above-obtained fundamental equation based on the Delaunay system is similar to the conventional one used so far.

2.4.2. Formulation for Voronoi system

Fig. 5 illustrates the finite difference grid for the Voronoi system. In contrast to the Delaunay mesh system, the material boundary in this case is located in between the grid points. So the material is divided into five blocks with permittivities denoted by $\epsilon_0 \sim \epsilon_4$, respectively. Also in this case, the basic Poisson equation is integrated using Gauss's theorem in the closed area surrounding a central node to result in the same eq. (8) mentioned above. What differs here is that the potential at the interface must be de-

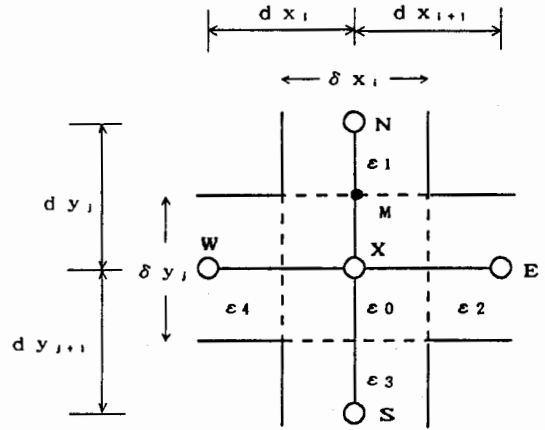


Fig. 5. The coordinate for 5-point FDM in Voronoi system.

rived before the integration can be performed. For this, let's define an "intermediate" node, denoted by M in fig. 4. Let ψ_M denote the potential at this intermediate node, one has for the first order derivative of ψ as follows.

$$\left. \frac{\partial \psi}{\partial y} \right|_{\text{region 0}} = \frac{\psi_M - \psi_X}{dy_j/2}, \quad (11-1)$$

$$\left. \frac{\partial \psi}{\partial y} \right|_{\text{region 1}} = \frac{\psi_N - \psi_M}{dy_j/2}. \quad (11-2)$$

Here, at the interface the boundary condition is satisfied by equation (7). Solution of (7) and (11) yields

$$\psi_M = \frac{\epsilon_0 \psi_X + \epsilon_1 \psi_N}{\epsilon_0 + \epsilon_1}. \quad (12)$$

Therefore, the five-point formulation for Voronoi system is written as follows.

$$\begin{aligned} 2\delta x_i \left\{ \frac{1}{dy_j} \left(\frac{\psi_N - \psi_X}{1/\epsilon_1 + 1/\epsilon_0} \right. \right. \\ \left. \left. + \frac{1}{dy_{j+1}} \left(\frac{\psi_E - \psi_X}{1/\epsilon_2 + 1/\epsilon_0} \right) \right\} \\ + 2\delta y_i \left\{ \frac{1}{dx_j} \left(\frac{\psi_S - \psi_X}{1/\epsilon_3 + 1/\epsilon_0} \right. \right. \\ \left. \left. + \frac{1}{dx_{i+1}} \left(\frac{\psi_W - \psi_X}{1/\epsilon_4 + 1/\epsilon_0} \right) \right\} \\ = \rho \delta x_i \delta y_j. \end{aligned} \quad (13)$$

The above new equation forms the basis for our method based on the Voronoi system.

2.5. Current continuity equation

The discretization formula between the grid points is given from the Scharfetter-Gummel scheme [9]. For fluids, this scheme is well known as an exponential method and the discretization error is comparable with that of the general formula for central finite difference. Because of this reason, the Scharfetter-Gummel scheme is selected for formulating the current continuity equations for holes and electrons. A five-point scheme applied to both Delaunay and Voronoi systems, yields the following equations for electron and hole continuity equations, respectively.

$$\begin{aligned} J_n = \mu_n \frac{\psi_X - \psi_N}{dy_j} \\ \times \left(\frac{n_X}{1 - \exp(\psi_X - \psi_N)} \right. \\ \left. + \frac{n_N}{1 - \exp(-(\psi_X - \psi_N))} \right), \end{aligned} \quad (14-1)$$

$$\begin{aligned} J_p = \mu_p \frac{\psi_X - \psi_N}{dy_j} \\ \times \left(\frac{p_X}{1 - \exp(-(\psi_X - \psi_N))} \right. \\ \left. + \frac{p_N}{1 - \exp(\psi_X - \psi_N)} \right), \end{aligned} \quad (14-2)$$

2.6. Simulation results

The sample device MOSFET for simulating the DC characteristic is an n-channel and polysilicon gate MOSFET. The mobility is taken as constant and no generation and recombination are accounted for. Fig. 6(a-c) and Fig. 7(a-c) indicate the internal potential, electron and hole distributions, respectively, which are simulated by Delaunay or Voronoi system at $VD = 5$ V, $VG = 5$ V, $VB = 0$ V. The potential distribution is as expected for the applied bias conditions. The electron distribution shows a channel formed at the interface between oxide and bulk silicon and extending from the source to the pinch-off point near the drain. The potential distribution also shows that holes are dominant in the region deep into the bulk.

Solutions obtained by Delaunay and Voronoi systems are in good agreement with each others.

Fig. 8 shows a drain current dependence on drain voltages as the gate voltage is kept constant at 1, 3 and 5 V, respectively.

By contrast, fig. 9 shows a drain current dependence on a gate voltages as the drain voltage is kept constant at 1 V.

Since the formulation based on the Delaunay system has been pointed out above to be similar to the conventional method, it can be concluded that the results obtained with the newly pro-

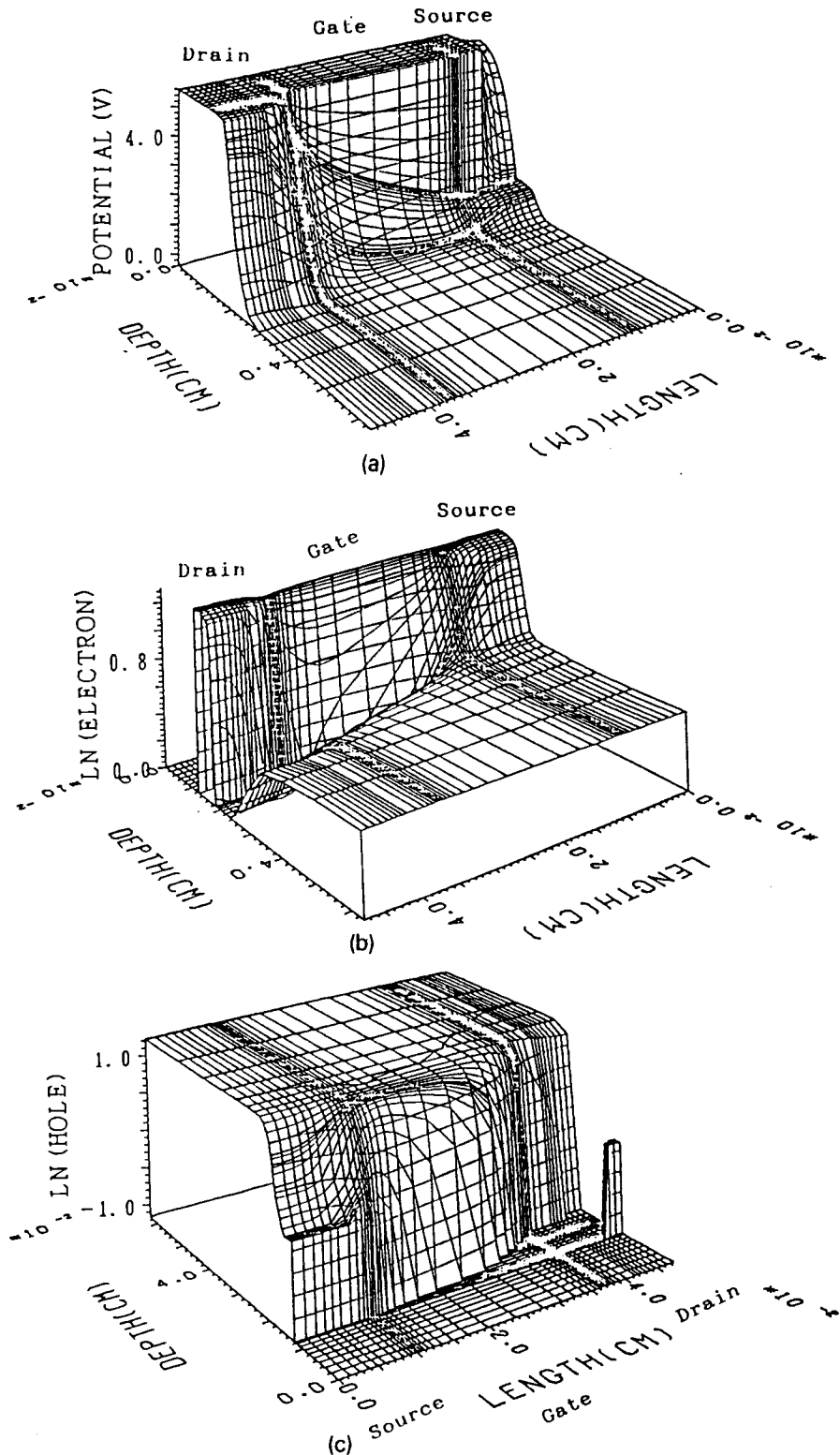


Fig. 6. Predicted distributions obtained by Delaunay system; (a) electrostatic potential, (b) electron concentration, (c) hole concentration.

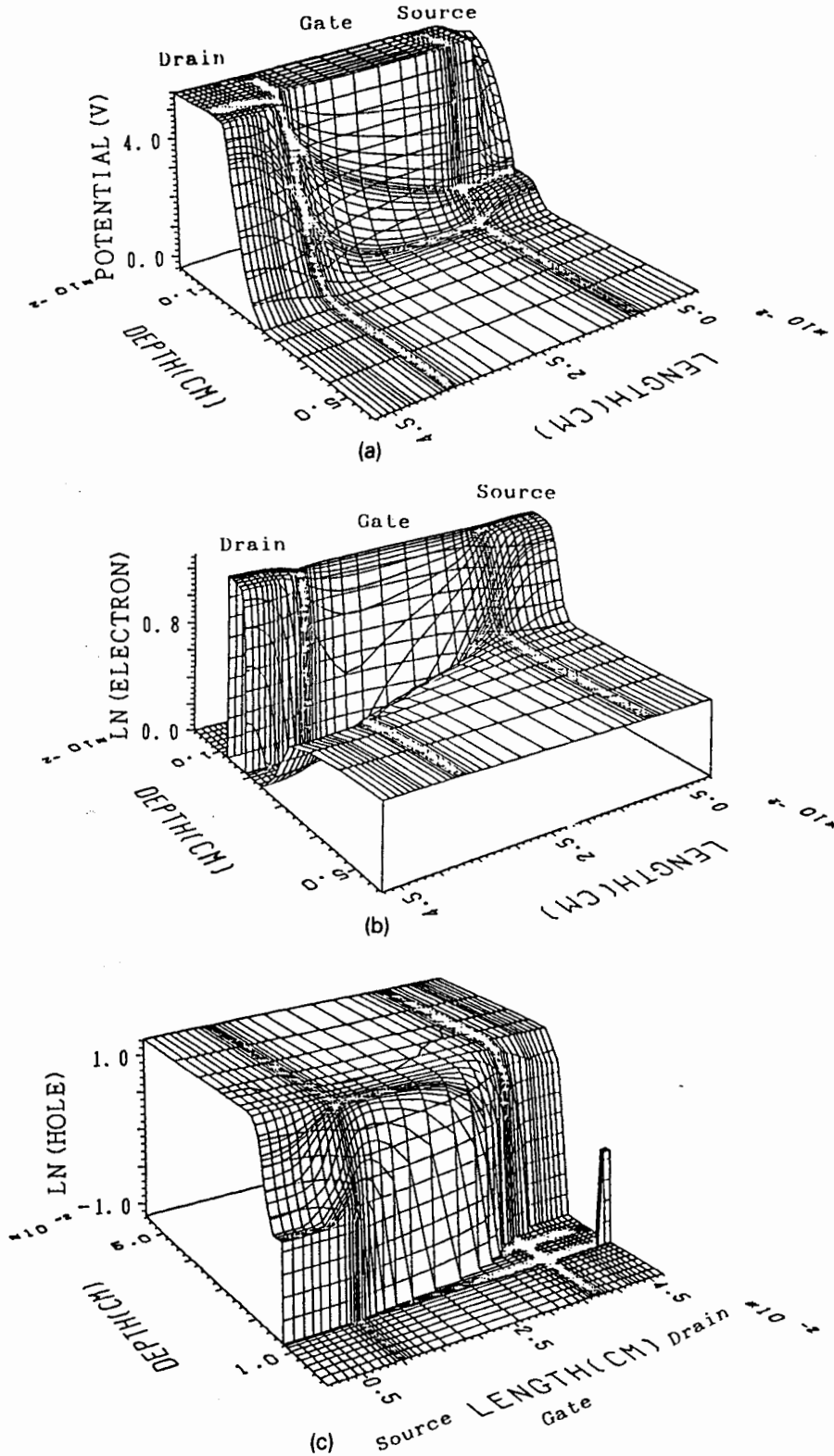


Fig. 7. Predicted distributions by Voronoi system; (a) electrostatic potential, (b) electron concentration, (c) hole concentration.

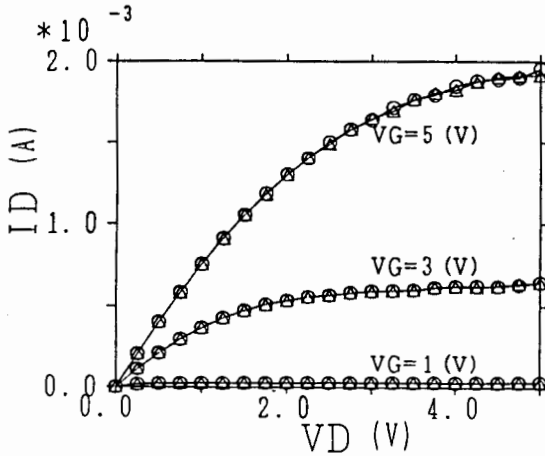


Fig. 8. Drain current versus drain voltage for a MOS transistor. Gate voltages are 1, 3 and 5 V respectively.

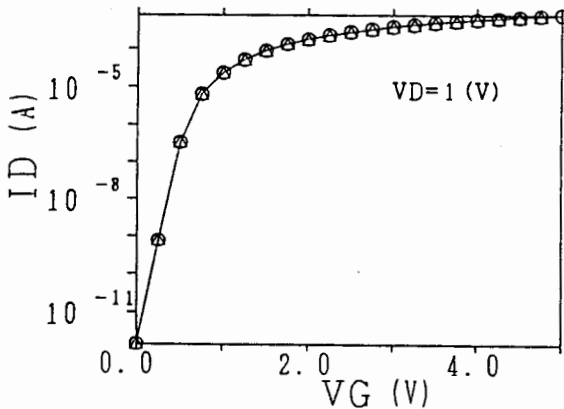


Fig. 9. Drain current versus gate voltage at drain voltage of 1 V.

posed Voronoi formulation are comparable to those of the conventional method in terms of accuracy. In other words, the newly developed method using two interlaced Voronoi and Delaunay systems, not only adds one more degree of freedom to the simulation of semiconductor devices, but can be expected to reduce computation cost as well. This latter problem will be considered at length in a coming paper.

3. Conclusion

A novel simulation method for semiconductor devices, is developed based on a discretization using two interlaced Voronoi-Delaunay mesh systems. The mathematical formulation, based on a five-point finite-difference method, applied to Poisson and electron and hole continuity equations, yields two sets of formulae: one for the Delaunay system is similar to the conventional model which has been widely used so far; the other for the Voronoi system is completely new. Excellent agreement is obtained between simulation results based on these two formulations.

As a conclusion, the newly developed Voronoi formulation has been proved to be an other effective simulation model adding more latitude to the analysis of semiconductor devices.

References

- [1] T. Wada and R. Dang, Development and application of a high-speed 2-dimensional time dependent device simulation (MOS2C), NASECODE-4 (1985) 108-119.
- [2] W. Engl, H.K. Dirks and B. Meinerzhagen, Device modeling, Proc. IEEE, vol. 71 (1967) 149-172.
- [3] C.S. Rafferty, M.R. Pinto and R.W. Dutton, Iterative methods in semiconductor device simulation, IEEE Trans. Electron Devices, vol. ED-32 (1983) 10-33.
- [4] J. Pennman and J.R. Fraser, Complementary and dual energy finite element principles in magnetostatics, IEEE Trans., Magn. MAG-18 (1982) 319-324.
- [5] P. Hammond and J. Pennman, Calculations of inductance and capacitance by means of dual energy principles, Proc. IEEE, vol. 123 (1976) 554-559.
- [6] Y. Saito, Y. Kishino, S. Hayano, H. Nakamura, N. Tsuya and Z.J. Cendes, Faster magnetic field computation using locally orthogonal discretization, IEEE Trans., Magn. MAG-22 (1986) 1057-1059.
- [7] T. Kojima, Y. Saito and R. Dang, Dual mesh approach for semiconductor device simulator, IEEE Trans., Magn. MAG-25 (1988) 2953-2955.
- [8] H.K. Gummel, Self-consistent iterative scheme for one-dimensional steady state transistor calculations, IEEE Trans. Electron Devices, ED-11 (1964) 455-465.
- [9] D.L. Scharfetter and H.K. Gummel, Large-signal analysis of silicon read diode oscillator, IEEE Trans., Electron Devices, E/D-16 (1969) 16-74.